Journal of Engineering and Applied Sciences 13 (15): 6188-6198, 2018
ISSN: 1816-949X

Design of an Adaptive Neural Voltage-Tracking Controller for Nonlinear Proton Exchange Membrane Fuel Cell System Based on Optimization Algorithms

Khulood E. Dagher
Al-Khwarizmi College of Engineering, University of Baghdad, Baghdad, Iraq

Abstract: This study proposes an enhancement for the performance of the neural voltage-tracking controller based on different types of on-line optimization algorithms for nonlinear Proton Exchange Membrane Fuel Cell (PEMFC) system. The goal of this research is to employ the NARMA-L2 neural model in order to identify and control the nonlinear system. The task of the proposed nonlinear adaptive neural inverse voltage-tracking controller is to find precisely and quickly the optimal hydrogen partial pressure action which is used to control the (PEMFC) stack terminal voltage. Three intelligent optimization algorithms are used to learn and tune the weights of the neural model, the first one is the FireFly Algorithm (FFA), the second one is the Chaotic Particle Swarm Optimization (CPSO) algorithm and the third one is the Hybrid Firefly-Chaotic Particle Swarm Optimization (HFF-CPSO) algorithm. The numerical simulation results show that the NARMA-L2 controller with (HFF-CPSO) algorithm is more accurate than CPSO and FFA in terms of quickly obtaining the neural controller's parameters with high reduction for the number of function evolutions and moreover in its capability of generating smooth partial pressure control response for the nonlinear (PEMFC) system without voltage oscillation in the output through investigating under random load-current variations.

Key words: Fuel cell system, adaptive inverse controller, NARMA-L2 neural network, chaotic particle swarm optimization, firefly algorithm, Iraq

INTRODUCTION

In general, the fuel cell operation looks like a battery operation where both of them convert the chemical energy produced from the chemical reaction into electricity. On the other hand, the DC electricity will be produced continuously in the fuel cell as long as the fuel (such as hydrogen) and an oxidant (such as oxygen) are supplied (plus water and heat) and this is the main difference between the fuel cell and the battery (Kumar *et al*., 2017). In fact, the fuel cell has several advantages such as the quiet operation and the zero emission, thus, it is cleaned by products water when operated on pure hydrogen and it also does not have any moving parts, even when it works with extra fuel processing and supply equipment. Furthermore, the fuel cell is better than the traditional combustion engine/generator sets, it has a high power density, high efficiency and the waste heat from a fuel cell can be used for heating purposes (Swain and Jena, 2015). This study deals with PEMFC Model only which is low temperature operating fuel cell designed or mass-production fuel cell vehicles and it is very preferable to be used in power automobiles, aircraft, homes and small offices as well as in portable electronics systems (Kandi *et al*., 2016). In the last decade, many control techniques and intelligent algorithms have been proposed to keep the fuel cell system working with the maximum power conversion such as traditional linear control techniques which convert the nonlinearity of the fuel cell system to the linear controller designs which are not effective when there is a large parameter variations and load disturbances (Manikandan and Ramalingam, 2016). Therefore, unconventional techniques with intelligent algorithms such as fuzzy-PID controller, predictive controller (Sedighizadeh *et al*., 2011), adaptive back-stepping controller (Zuniga-Ventura *et al*., 2015) and sliding mode controller (Derbeli *et al*., 2017; Jiao, 2013) were adopted also, many types of intelligent evolutionary algorithms have been used to build the modelling of PEMFC and controlling it such as genetic algorithm (Kumar *et al*., 2017; Rajasekar *et al*., 2015), artificial bees colony optimization (Safavi, 2013), particle swarm optimization algorithm and firefly optimization algorithm (Nazarian and Hadidian-Moghddam, 2015). In this study, the Nonlinear Auto-Regressive Moving Average (NARMA) neural network control algorithm has been designed based on the identification technique for the nonlinear mathematical model of the PEMFC system. This control algorithm is proposed to improve the dynamic behavior of the output voltage of the fuel cell through

generating an optimal hydrogen partial pressure control action. The fuel cell's dynamic response is of significant importance, particularly in mobile applications. Therefore, the main motivations of this work are to address the issue of PEMFC slow transient response to load current changes which is very important, since, the dynamic behavior of a fuel cell is integral to the overall stability and performance of the power system formed by the fuel cell stack. Furthermore, the modeling and controlling for the nonlinear PEMFC system are still challenging. The contribution of this research is the design of an adaptive inverse neural voltage-tracking controller based on NARMA-L2 with a new hybrid FireFly-Chaotic Particle Swarm Optimization (FFCPSO) in order to improve the dynamic performance of modeling and controlling of the nonlinear PEMFC system as well as it is more accurate compared to another neural control algorithm in terms of: fast learning, no oscillation in the output and minimum number of fitness evaluation.

Nonlinear model of PEM fuel cell: In 1960's General Electric in the United States developed the PEMFC which is also known aspolymerfuel cell to be used by NASA on their first manned space vehicles (Damour *et al*., 2014). Figure 1 shows the reaction diagram of PEMFC. Mostly this kind of cell depends on a special polymer membrane coated with highly dispersed catalyst particles. The hydrogen is fed to the membrane's anode side where the catalyst causes the hydrogen atoms to release their electrons and become H^+ ions (protons) (El-Sharkh *et al*., 2004; Seyezhai, 2015):

$$2H_2 \rightarrow 4H^+ + 4e^- \quad (1)$$

Only H^+ ions pass through the Proton Exchange Membrane (PEM) while the electrons are travelled to an external circuit to generate the electrical output, before reaching the cathode side. The electrons and the hydrogen ions combine with the supplied oxygen from air to form water, this reaction releases energy in heat form (Mammar and Chaker, 2009):

$$4e^- + 4H^+ + O_2 \rightarrow 2H_2O \quad (2)$$

The produced water must be expelled to prevent cell from flooding and rendering inoperative. The reaction in a single fuel cell produces an output voltage of around 0.7 V for general applications, a fuel cell stack is used which represents several individual cells connected in series to produce the desired voltage additively. The required operating temperature for PEMFCs is only 50-100°C which enables fast start-up of operation (Correa *et al*., 2003). In general, the polarization curve is used to express the fuel cell performance and this

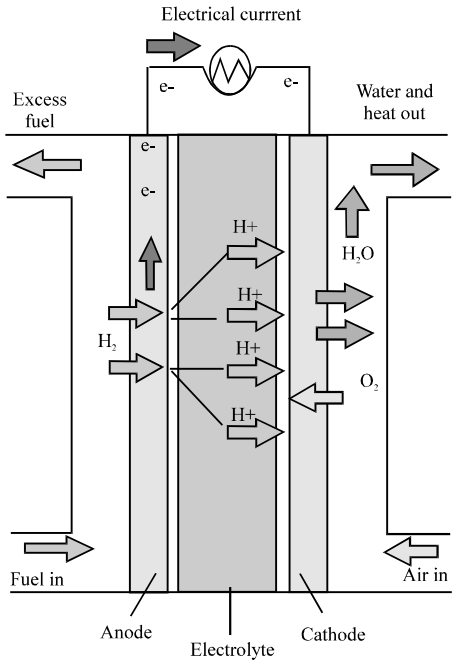

Fig. 1: The schematic diagram of PEMFC reaction

curve shows highly nonlinear characteristics between Voltage-load current (V-I) (El-Sharkh *et al*., 2004; Seyezhai, 2015). Therefore, the modeling of the V-I characteristics of fuel cells is very important. For PEM fuel cells the steady-state V-I characteristics of a fuel cell can be determined by El-Sharkh *et al*. (2004) and Seyezhai (2015):

$$V_{cell}(t) = V_{steady\_component} - V_{transient\_component} \quad (3)$$

$$V_{steady\_component} = E_N - V_{ohmic} \quad (4)$$

$$V_{transient\_component} = V_{activation} + V_{concentration} \quad (5)$$

Where:

V_{cell} = The fuel cell output voltage

E_N = The fuel cell reversible voltage

V_{ohmic} = The ohmic voltage drops resulting from the resistance of the conduction of protons through the solid electrolyte and of the electrons through its path

$V_{activation}$ = The drop voltage due to the activation of the anode and cathode

$V_{concentration}$ = The drop voltage resulting from the reduction in concentration of the reactant's gases or from the transport of mass of oxygen and hydrogen

Table 1: The parameters of the fuel cell

Parameters	Values	Units
Ncell	32	-
T	333	Kelvin degree (K)
A	64	cm^2
l	178	cm
P_{H2}	1-5	atm
P_{O2}	0.2095	Atm
R_C	0.0003	Ω
β	0.016	V
α_1	-0.948	-
α_2	0.00312	-
α_3	7.6×10^{-5}	-
α_4	-1.93×10^{-4}	-
J	7	mA/cm^2
J_{max}	0.469	A/cm^2
ϕ	20	-

Each term in Eq. 3-5 can be calculated by using the parameters listed in Table 1 (Correa *et al*., 2003) and its own law as follows:

The reversible cell potential (E_N) is the cell electrochemical thermodynamics potential and it represents the ideal output voltage and can be calculated as follows (Correa *et al*., 2003):

$$E_N = 1.229-0.85.10^{-3}\times(T-298)+4.3085.10^{-5}\times (T.(\ln(P_{H2})+0.5\ln(P_{O2})) \quad (6)$$

The activation over voltage is the voltage drop due to the activation of the anode and the cathode and can be expressed as follows (El-Sharkh *et al*., 2004; Seyezhai, 2015):

$$V_{activation} = \alpha_1+\alpha_2.T+\alpha_3.T.\ln(C_{O2})+\alpha_4.T.\ln(I) \quad (7)$$

Where:

I = Cell loaded current

C_{O2} = The dissolved oxygen concentration in the cathode catalytic surface in mol/cm^3

By using the Henry law Co_2 derived from partial pressure of the oxygen and temperature of the cell by El-Sharkh *et al*. (2004) and Seyezhai (2015):

$$C_{o2} = \frac{P_{O2}}{5.08\times10^6.\exp\left(\frac{-498}{T}\right)} \quad (8)$$

The Ohmic polarization loss is calculated by Eq. 9 (Swain and Jena, 2015):

$$V_{ohmic} = I.(R_c+R_m) \quad (9)$$

Where:

R_m = The electron flow equivalent resistance

R_c = A constant value to represent the proton resistance

$$R_m = \frac{\rho_m l}{A} \quad (10)$$

where, ρ_m is the membrane (Ω cm) specific resistance and can be formulated as following (Derbeli *et al*., 2016):

$$\rho_m = \frac{181.6\left[1+0.03\left(\frac{1}{A}\right)+0.062\left(\frac{T}{303}\right)^2\left(\frac{1}{A}\right)^{2.5}\right]}{\left[\varphi-0.634-3\left(\frac{1}{A}\right)\exp^{[4.18(T-303)/T]}\right]} \quad (11)$$

where, φ is an adjustable parameter of the humidity condition. During the reaction, there is a reactant concentration drop (oxygen and hydrogen) which is called the concentration loss and it can be calculated by the chemical reaction loss of Eq. 12 (El-Sharkh *et al*., 2004; Seyezhai, 2015):

$$V_{concentration} = -\beta.\ln\left(1-\frac{J}{J_{max}}\right) \quad (12)$$

Where:

β = Cell typed dependence parameter

J = The density of the current which passes through the cell (A/cm^2)

J_{max} = The maximum current density that passes through the cell (A/cm^2)

It can be calculated by using Eq. 13:

$$J_{max} = \frac{I_{max}}{A} \quad (13)$$

So, the output voltage of the fuel-cell stack is calculated by the following Eq. 14 (El-Sharkh *et al*., 2004; Seyezhai, 2015):

$$V_{FC} = N_{cell}V_{cell} \quad (14)$$

where, N_{cell} is the fuel cell number in stack. The total power density provided by the fuel cell to the load can be determined by Eq. 15:

$$Power_{FC} = I.V_{FC} \quad (15)$$

MATERIALS AND METHODS

Neural inverse controller design: The main task of the proposed adaptive neural inverse controller is to generate precisely and quickly the optimal hydrogen partial pressure action in order to control the voltage of the stack

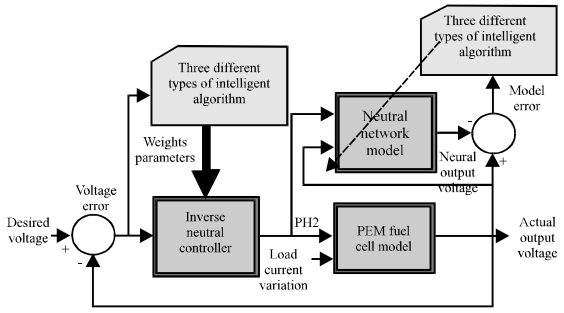

Fig. 2: The proposed neural controller structure

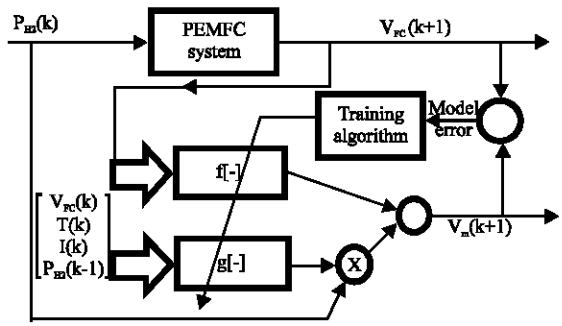

Fig. 3: The NARMA-L2 Model structure with serial-parallel configuration

terminal in PEMFC Model. The general structure of the proposed neural inverse voltage tracking controller is shown in Fig. 2. There are two steps towards designing the proposed adaptive neural inverse controller:

First step: In this step, the identification technique is used to build the PEMFS Model based on NARMA-L2 neural network. The structure of the Nonlinear Auto Regressive Moving Average-Linear 2 (NARMA-L2) model based on MultiLayer Perceptron (MLP) neural networks with serial-parallel configuration is shown in Fig. 3 (Fourati *et al*., 2015; Kananai and Chancharoen, 2012). The proposed equation of the NARMA-L2 Model based on the fuel-cell stack output voltage V_{FC} and the temperature variable T of the fuel cell system the load current variation I and the hydrogen partial pressure P_{H2} controlled effort can be formulated as follows:

$$V_{FC}(k+d) = f\begin{bmatrix} V_{FC}(k),...,V_{FC}(k\text{-}n+1),T(k),... \\ T(k\text{-}n+1),I(k),...,I(k\text{-}n+1),P_{H2} \\ (k\text{-}1),...,P_{H2}(k\text{-}n+1) \end{bmatrix} + g\begin{bmatrix} V_{FC}(k),...,V_{FC}(k\text{-}n+1),T(k),...,TV_{FC}(k\text{-}n+1), \\ I(k),...,IV_{FC}(k\text{-}n+1),P_{H2}(k\text{-}1),...,P_{H2}V_{FC}(k\text{-}n+1) \end{bmatrix} \times P_{H2}(k) \quad (16)$$

where, f[-] and g[-] are the functions of the past values of input-output of the fuel cell system. The mean square error function is used as the objective cost function in learning algorithm in order to minimize the error between the actual output of the fuel cell and the output of the neural network as in Eq. 17 by using Eq. 18 (Zurada, 1992):

$$e(k+1) = V_{FC}(k+1) - V_m(k+1) \quad (17)$$

$$E = \frac{1}{np}\sum_{i=1}^{np}\left(e^i(k+1)\right)^2 = \left(\frac{1}{np}\right) \sum_{i=1}^{np} V_{FC}^i(k+1) - V_m^i(k+1)^2 \quad (18)$$

Where:

np = The number of population
e^i = The error of each iteration
V^i_{FC} = The actual output voltage of the fuel cell of each iteration
V^i_m = The model output voltage of the neural network of each iteration

After applying the training mechanism of the neural network as shown in Fig. 2 by using intelligent optimization algorithms in order to reduce the error between the actual output voltage $V_{FC}(k+1)$ and neural network model output voltage $V_m(k+1)$ and is equal to zero approximately then the model will complete the same actual output response. When identification of the plant is complete, then g[-] can be approximated by $\hat{g}$[-] and f[-] by $\hat{f}$[-] and the NARMA-L2 Model of the stack fuel cell can be described in Eq. 19:

$$V_m(k+1) = \hat{f}\begin{bmatrix} V_{FC}(k),...,V_{FC}(k\text{-}n)+1,T(k),... \\ T(k\text{-}n+1),I(k),...,I(k\text{-}n+1),P_{H2} \\ (k\text{-}1),...,P_{H2}(k\text{-}n+1) \end{bmatrix} + \hat{g}\begin{bmatrix} V_{FC}(k),...,V_{FC}(k\text{-}n+1),T(k),...,T(k\text{-}n+1), \\ I(k),...,I(k\text{-}n\text{-}1),P_{H2}(k\text{-}1),...,P_{H2}(k\text{-}n+1) \end{bmatrix} \times P_{H2}(k) \quad (19)$$

Therefore, the control law of the adaptive inverse neural voltage tracking controller can be obtained from the Jacobian that can be defined as the $\hat{g}$[-] neural network and it has the sign definite in the fuel cell operation region in order to guarantee the uniqueness of the fuel cell inverse at that operating region:

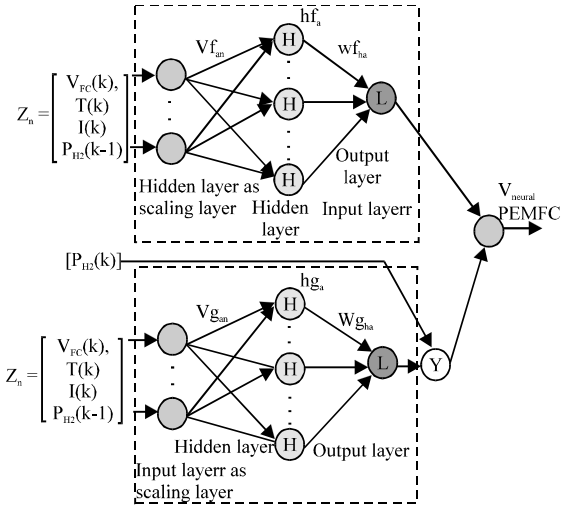

Fig. 4: The structure of both $\hat{f}[\cdot]$ and $\hat{g}[\cdot]$ neural network

$$P_{H2}(k+1) = \frac{V_{des}(k+1) - \hat{f}\begin{bmatrix} V_{FC}(k),...,V_{FC}(k-n+1),T(k) \\ ,...,T(k-n+1),I(k),...,I \\ (k-n+1),P_{H2}(k-1),...,P_{H2} \\ (k-n+1) \end{bmatrix}}{\hat{g}\begin{bmatrix} V_{FC}(k),...,V_{FC}(k-n+1),T(k),... \\ T(k-n+1),I(k),...,I(k-n-1), \\ P_{H2}(k-1),...,P_{H2}(k-n+1) \end{bmatrix}} \quad (20)$$

where, $V_{des}(k+1)$ denotes the desired output voltage value of the fuel cell. The neural network structure $\hat{f}[\cdot]$ and $\hat{g}[\cdot]$ are the Multi-Layer Perceptron (MLP) Model and each one consists of three layers: the input or buffer layer, the hidden or activation layer and the output layer (Zurada, 1992; Nells, 2001) as shown in Fig. 4. So, the network weights of the $\hat{f}[\cdot]$ and $\hat{g}[\cdot]$ can be illustrated as follows:

Vf_{an} = The weight matrix of the $\hat{f}[\cdot]$ hidden layer
Wf_{ba} = The weight matrix of the $\hat{f}[\cdot]$ output layer
Vg_{an} = The weight matrix of the $\hat{g}[\cdot]$ hidden layer
Wg_{ba} = The weight matrix of the $\hat{g}[\cdot]$ output layer

To describe the calculations of neuron in the hidden layer, firstly, we will sum the net of the weights Vf_{an} and Vg_{an} by using Eqs. 21 and 22 (Zurada, 1992; Nells, 2001):

$$netf_a = \sum_{a=1}^{nh} Vf_{an} \times \overline{Z_n} \quad (21)$$

$$netg_a = \sum_{a=1}^{nh} Vg_{an} \times \overline{Z_n} \quad (22)$$

where, nh is the hidden nodes number. Secondly, the neuron outputs of both hf_a and hg_a are calculated as a continuous unipolar sigmoSid activation function of the $netf_a$ and $netg_a$ as in Eq. 23 and 24, respectively (Zurada, 1992; Nells, 2001):

$$H(netf_a) = \frac{1}{1+e^{-netf_a}} \quad (23)$$

$$H(netg_a) = \frac{1}{1+e^{-netg_a}} \quad (24)$$

Thirdly, to calculate the weighted sum $netf_o$ and $netg_o$ of the output layers, Eq. 25 and 26 are used, respectively:

$$netfo_b = \sum_{a=1}^{nh} Wf_{ba} \times \overline{hf_a} \quad (25)$$

$$netgo_b = \sum_{a=1}^{nh} Wg_{ba} \times \overline{hg_a} \quad (26)$$

The one linear neuron passes the sum of both ($netfo_b$) and ($netgo_b$) through a linear function of slope 1 as in Eq. 27 and 28:

$$Of_b = L(netfo_b) \quad (27)$$

$$Og_b = L(netgo_b) \quad (28)$$

Second step: This step describes the use of different types of the intelligent algorithms in order to find and tune the best weights neural controller and show the effectiveness of them in terms of number of iterations for evaluating the fitness function and the minimum value obtained for the cost function.

The firefly algorithm: One of the meta-heuristic algorithms is the firefly algorithm and the principle of operation of this algorithm is based on the fireflies flashing behavior (Abdelaziz *et al*., 2015). In general, the firefly algorithm formulation is based on three ideal rules: the 1st one is that all fireflies are unisex, the 2nd rule is that the firefly attractiveness (β) is proportional to the brightness (I) and if the brightness of both fireflies decreases that means the distance (r) between them is increased. The 3rd rule is that in the firefly movement, the less bright one will move towards the brighter one and if there is no brighter one than a particular firefly that means the firefly will move randomly. The brightness have to be associated with the objective function. The relationship between the attractiveness of each firefly described by monotonically decreasing function of the distance

between any two fireflies can be formulated as follows (Nazarian and Hadidian-Moghddam, 2015; Abdelaziz *et al*., 2015):

$$\beta = \beta_0 \exp^{-\gamma r^m} \quad (29)$$

where, β_0 is equal to 1 and it represents the maximum attractiveness (at r = 0). γ is a factor with the range from 0.1-10 and it represents the light absorption. m is more than 1.

The distance between any two fireflies (i) and (j) at positions x_i and x_j is estimated using the distance formula as follows (Nazarian and Hadidian-Moghddam, 2015; Abdelaziz *et al*., 2015):

$$r_{ij} = \sqrt{\sum_{k=1}^{d}\left(x_{i,k}-x_{j,k}\right)^2} \quad (30)$$

where, d denotes the number of dimensions. $X_{i,k}$ is the kth spatial coordinate element kth of ith firefly.

The firefly i movement can be formulated as three terms: the first one represents firefly current location, the other one represents the firefly's attractiveness and the final one denotes the random movement of the firefly if there are no brighter fireflies (Nazarian and Hadidian-Moghddam, 2015; Abdelaziz *et al*., 2015):

$$x_i = x_i + \beta_0 \exp^{-\gamma r^m}\left(x_i - x_j\right) + \propto \left(\text{rand}-0.5\right) \quad (31)$$

where, α is a randomization variable between (0-1).

Particle swarm and chaotic particle swarm optimization algorithms: In general, one of the modern stochastic search algorithms is the Particle Swarm Optimization (PSO) which is famous by its simple concept, easy implementation and quick convergence (Rini *et al*., 2011). This technique particles start at a random initial particle (population of individuals) each particle is leaded by the internal interaction in order to get the near optimal solution by minimizing or maximizing a given objective function by flying through the search space. The movement of particle i, x_i, depends on its velocity, V_i which is adjusted at each time step by using the global best position, G_{best} and the local best position, L_{best} which have been already found. Equation 32 represents the particle's velocity update and Eq. 33 represents the particle's position update (Rini *et al*., 2011):

$$v_i(k+1) = w.v_i(k) + c_1 r_1\left[L_{best-i} - x_i(k)\right] + c_2 r_2\left[G_{best} - x_i(k)\right] \quad (32)$$

$$x_i(k+1) = x_i(k) + v_i(k+1) \quad (33)$$

where c_1 and c_2 are cognitive coefficients and r_1 and r_2 are two uniform random numbers from (0-1). In order to solve global optimization problems with a large number of local minima, the chaotic technique is used because it has been exploited in some metaheuristic methods which makes it generally exhibits better numerical performance than random operators in searching (Chauhan *et al*., 2015).

Therefore, Chaotic Particle Swarm Optimization (CPSO) algorithm is proposed in this research because it has ability to improve the global searches and reach to optimal solution with minimum number of iterations that depend on probabilities of the chaotic techniques (Dong *et al*., 2016) than stochastic techniques. The logistic equation employed for constructing chaotic PSO is described as Chauhan *et al*. (2015):

$$\beta(k+1) = \mu\beta(k)\left[1-\beta(k)\right] \quad (34)$$

where, μ is equal to 4 as the control parameter therefore, $(0) \notin \{0, 0.25, 0.5, 0.75, 1\}$. To calculate the new weight parameter w_{new}, Eq. 34 and 35 are used as follows:

$$w = w_{max} - \left[\left(w_{max} - w_{min}\right) \times \frac{\text{iteration}(k)}{\text{max.no.iteration}}\right] \quad (35)$$

$$w_{new} = \beta(k+1)w \quad (36)$$

To enhance the capability of PSO in the global searching, it has to put the new inertia weighting in the velocity update equation and it becomes as follows:

$$v_i(k+1) = w_{new}.v_i(k) + c_1 r_1\left[L_{best-i} - x_i(k)\right] + c_2 r_2\left[G_{best} - x_i(k)\right] \quad (37)$$

The proposed hybrid optimization algorithm: The proposed algorithm combines two optimization algorithms, namely the firefly and the CPSO in order optimization in order to increase the speed of learning, avoid filling in the local minimum and reduce the number of fitness evaluation. The hybrid FFCPSO algorithm develops the movement of the firefly equation by converting the equation of the distance forms as the distance between x_i and L_{best} in the Cartesian distance as in Eq. 38 as well as the distance between x_i and G_{best} in the Cartesian distance as in Eq. 39:

$$r_{Lx} = \sqrt{\sum_{k=1}^{d}\left(L_{best\text{-}i,j} - x_{i,j}\right)^2} \quad (38)$$

$$r_{Gx} = \sqrt{\sum_{k=1}^{d}\left(G_{best\text{-}i,j} - x_{i,j}\right)^2} \quad (39)$$

Also, the new inertia weighting as in Eq. 36 is added to the movement of a firefly equation, then the final proposed movement of a firefly can be represented as follows:

$$x_i(k+1) = w_{new}.x_i(k) + c_1 \exp^{-r_{Lx}^m}\left(L_{best-i} - x_i(k)\right) + c_2 \exp^{-r_{Lx}^m}\left(G_{best-i} - x_i(k)\right) + \propto (rand - 0.5) \quad (40)$$

So, the effectiveness of the proposed hybrid FFCPSO algorithm shows in the entire population, each particle is randomly attracted towards the G_{best} position and the local search in different regions is carried out by the modified attractiveness step of the proposed algorithm.

RESULTS AND DISCUSSION

To apply the proposed inverse neural voltage-tracking controller structure on PEMFC system as shown in Fig. 2, the numerical simulation is done by applying MATLAB package. The first step is to execute the identification technique in order to construct the model of the PEMFC based on NARMA-L2 neural network by using three different types of the intelligent learning algorithms that were explained in section three. The second step is to implement the inverse neural network controller design in order to precisely and quickly obtain the optimal hydrogen partial pressure action to control the (PEMFC) stack terminal voltage. To show the output voltage of cell static operation against the load current of the fuel cell, the polarization curve is important because it shows how the fuel cell voltage behaves when the load current changes as shown in Fig. 5 by using Eq. from 3-15 and the data in Table 1 with hydrogen and air of pressure 1 atm and at a temperature of 25°C with the maximum current for this stack which is 30 A. The loss voltage of the fuel cell can be shown in Fig. 6. Figure 7 shows the temperature effect on the polarization curve of the full cell when it changes from 25-55°C. Figure 8 shows the stack output power against the current and the maximum power is clear at the current which is equal to 29 A. There are 100 samples as inputs (hydrogen partial pressure, load current and temperature) output as (voltage) to neural PEMFC model and these inputs are chosen as Pseudo Random Binary Sequence (PRBS) signals with high-frequency and low-amplitude change

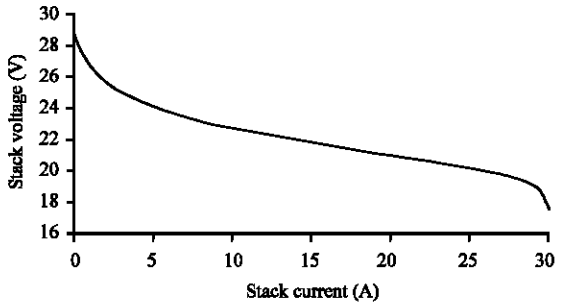

Fig. 5: The polarization curve

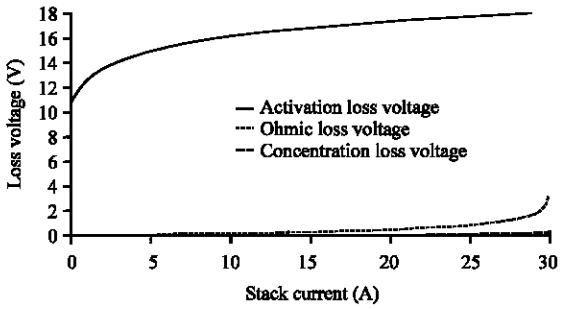

Fig. 6: The loss voltage of the fuel cell

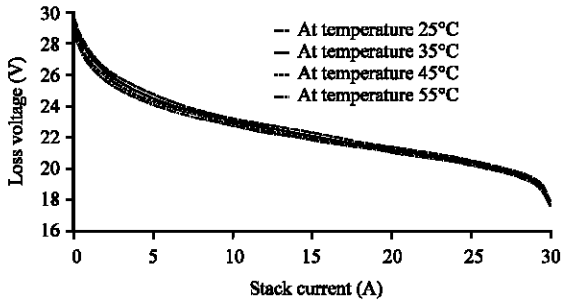

Fig. 7: The polarization curve of the full cell for different temperature operations

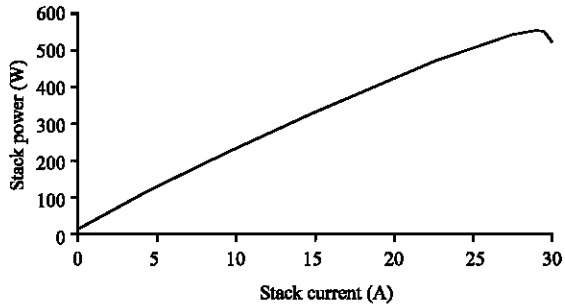

Fig. 8: The stack output power against the current

with a mean value whih is equal to zero in order to excite all nonlinear regions of the PEMFC system in the open loop step changes as shown in Fig. 9-a-d, respectively.

Table 2: Parameters of different types of intelligent algorithms

Algorithm type	No. of particles	No. of firefly	Particle's weights	Firefly's weights	[β, γ, α, m]	c_1 and c_2	r_1 and r_2	The best number of iteration
CPSO	50		220		-	1.25	Random (0,1)	85
FF	-	50	-	220	[1,5, 0.2, 2]	-	-	110
FFCPSO	-	50		220	[-,-,0.2,-]	1.25	-	45

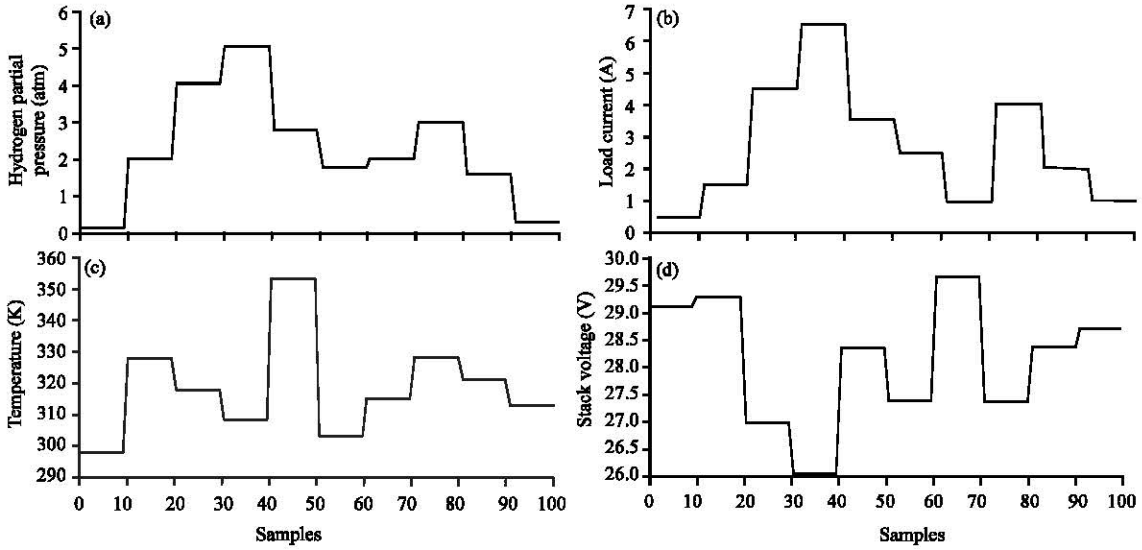

Fig. 9: a) The input signal hydrogen partial pressure used to excite the PEMFC system; b) The input signal load current used to excite the PEMFC system; c) The input signal temperature used to excite the PEMFC system and d) The open loop response of the PEMFC to the PRBS input signals

Based on these figures, there is an essential need for adding a scaling function in the input layer of the neural network model in order to avoid numerical errors in the activation function of the hidden layer. Moreover, it is important to add a scaling function in the output layer of the neural netork model because the output voltage is between 26-30 V. Based on the stack voltage equation of the PEMFC system, we proposed the dynamic model of the PEMFC system as Eq. 19 that has a 3rd order system dynamic behavior as follows:

$$V_m(k+1) = \hat{f}\begin{bmatrix} V_{FC}(k), V_{FC}(k-1), V_{FC}(k-2), \\ T(k), T(k-1), I(k), I(k+1), \\ P_{H2}(k-1), P_{H2}(k-2) \end{bmatrix} + \hat{g}\begin{bmatrix} V_{FC}(k), V_{FC}(k-1), V_{FC}(k-2), T(T), T(k-1), \\ I(k), I(k+1), P_{H2}(k-1), P_{H2}(k-2)\times P_{H2}(k) \end{bmatrix} \quad (41)$$

Since, each of $\hat{f}[\cdot]$ and $\hat{g}[\cdot]$ has nine inputs based on Eq. 41, the nodes in the NARNA-L2 neural network structure based on MLP are proposed as [9:11:1], representing the number of nodes in the input layer, the number of nodes in the hidden layer and the number of nodes in the output layer, respectively.

During the learning cycle of the PEMFC neural network model based on three different types of intelligent algorithms, Table 2 shows these parameters. The responses of neural PEMFC Models with three different types of the intelligent algorithms are shown in Fig. 10 where it shows the excellent response of the neural PEMFC Model with the actual output voltage of the PEMFC for the 100 patterns using the learning FFCPSO algorithm due to the minimum number of iterations and the minimum value of the performance index as shown in Fig. 11.

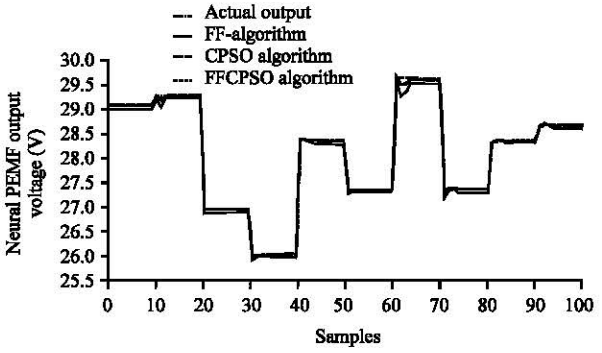

Fig. 10: The responses of neural PEMFC Models with the actual output voltage for three types of intelligent algorithms for learning patterns

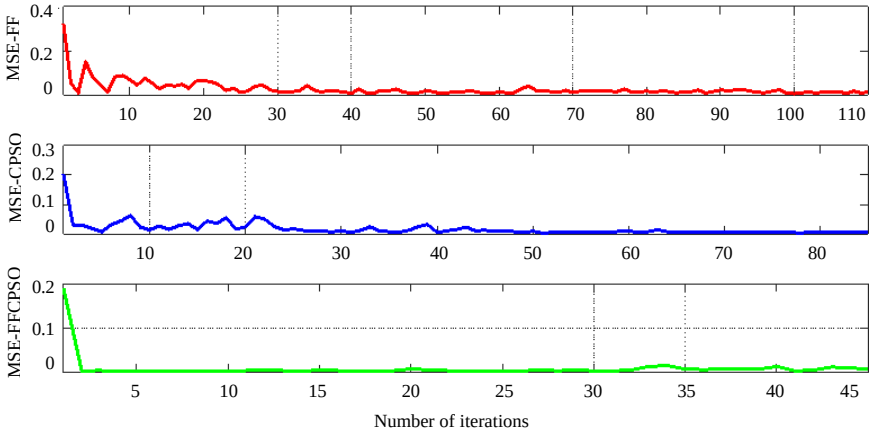

Fig. 11: The performance index for three different types of optimization algorithms

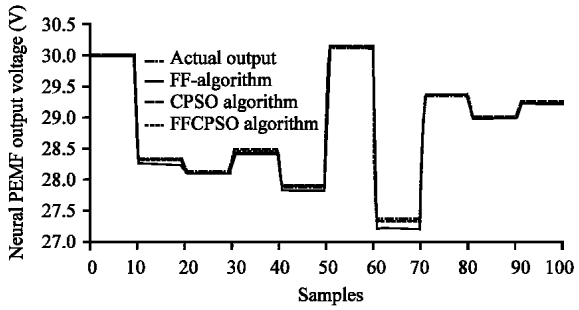

Fig. 12: The responses of neural PEMFC Models with the actual output voltage for three types of intelligent algorithms for testing patterns

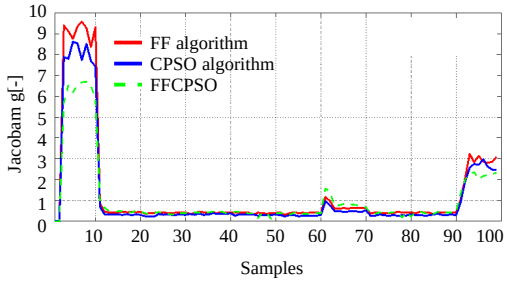

Fig. 13: The Jacobain of the neural PEMFC Models for learning pattern

Figure 12 shows the responses of neural PEMFC Model with three different types of the intelligent algorithms for 100 patterns as a testing set, it can be observed that all neural network models for the PEMFC system followed the PEMFC actual output voltage without the over learning problem occurred in the training cycle for all learning algorithms.

Figure 13 shows the Jacobian of the neural PEMFC model with three different types of optimization algorithms, so, it is observed that $\hat{g}[-]$ is sign definite in all

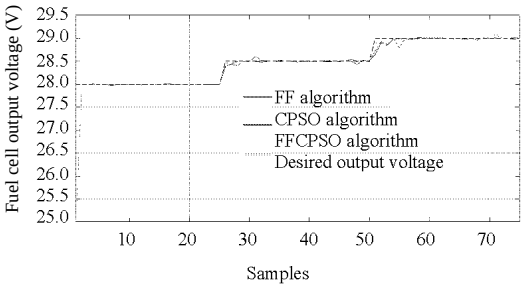

Fig. 14: The actual PEMFC response

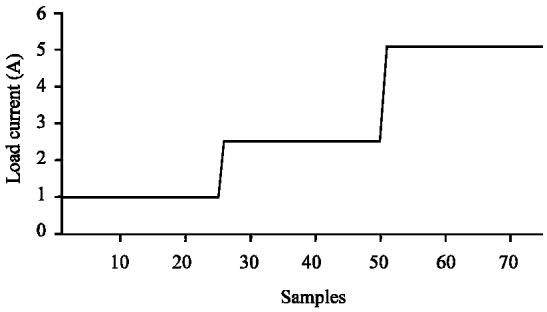

Fig. 15: The load current variation

the region of work interest which means that the models are invertable and can implement Eq. 20 for the inverse neural controller for the PEMFC system.

Figure 14 shows the three different step change desired outputs voltages with three cases variable load current (1, 2.5, 5) A as shown in Fig. 15 during 75 samples. Three responses of the PEMFC output voltage after applying the three neural PEMFC models as inverse neural controllers are based on the structure of NARMA-L2 Model with three different types of the tuning algorithms. Each inverse neural controller has the ability for tracking the desired output voltage with variable load current. However, the best performance of

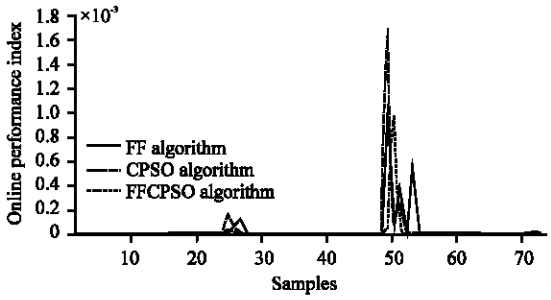

Fig. 16: The performance index for three different types of optimization algorithms during tuning weights parameters of the controller

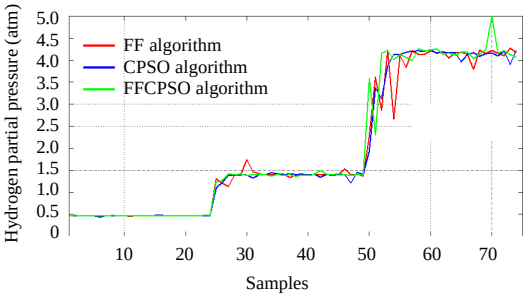

Fig. 17: The hydrogen partial pressure control signal based on three different types of the intelligent algorithms

the controllers is for the neural PEMFC Model that was learned by FFCPSO algorithm. It is observed that, the actual output voltage of the PEMFC is excellently tracking the desired output voltage and it has small overshoot without oscillation in the output. This controller is more accurate and the steady state error is equal to zero approximation with a minimum value of the on-line performance index as shown in Fig. 16, compared with the inverse neural controller based FF algorithm and CPSO algorithm. Figure 17 shows the hydrogen partial pressure control action of the inverse neural controller which has a small spike action of the partial pressure to track the desired output voltage and it approximately minimizes the steady state error to the zero value.

CONCLUSION

The numerical simulation results of the proposed Hybrid Firefly-Chaotic Particle Swarm Optimization (HFF-CPSO) algorithm with neural network NARMA-L2 Model are presented in this study for modelling and controlling the nonlinear PEMFC system. The proposed learning algorithm has many abilities when compared with firefly algorithm and chaotic particle swarm optimization algorithm in terms of, strong learning algorithm to build neural network model without over-learning problem, minimum fitness evaluation needed to find the optimal weight parameters of the neural model, fast and smooth learning algorithm which leads to no oscillation in the output neural model, robust inverse neural controller tuning parameters that generate the hydrogen partial action to track the desired output voltage of the PEMFC system during the load current variation.

REFERENCES

Abdelaziz, A., S. Mekhamer, M. Badr and M. Algabalawy, 2015. The firefly metaheuristic algorithms: Developments and applications. Intl. Electr. Eng. J., 6: 1945-1952.

Chauhan, P., M. Pant and K. Deep, 2015. Parameter optimization of multi-pass turning using chaotic PSO. Intl. J. Mach. Learn. Cybern., 6: 319-337.

Correa, J.M., F.A. Farret, J.R. Gomes and M.G. Simoes, 2003. Simulation of fuel-cell stacks using a computer-controlled power rectifier with the purposes of actual high-power injection applications. IEEE. Trans. Ind. Appl., 39: 1136-1142.

Damour, C., M. Benne, B. Grondin-Perez and J.P. Chabriat, 2014. Neural model-based self-tuning PID strategy applied to PEMFC. Eng., 6: 159-168.

Derbeli, M., M. Farhat, O. Barambones and L. Sbita, 2017. Control of PEM fuel cell power system using sliding mode and super-twisting algorithms. Intl. J. Hydrogen Energy, 42: 8833-8844.

Dong, N., X. Fang and A.G. Wu, 2016. A novel chaotic particle swarm optimization algorithm for parking space guidance. Math. Prob. Eng., 2016: 1-14.

El-Sharkh, M.Y., A. Rahman and M.S. Alam, 2004. Neural networks-based control of active and reactive power of a stand-alone PEM fuel cell power plant. J. Power Sources, 135: 88-94.

Fourati, F., S. Baklouti and H. Moalla, 2015. NARMA-L2 neural control of a bioreactor. Proceedings of the 4th International Conference on Systems and Control (ICSC'15), April 28-30, 2015, IEEE, Sousse, Tunisia, ISBN:978-1-4673-7108-7, pp: 504-509.

Jiao, J., 2013. Sliding mode control for stabilizing of boost converter in a solid oxide fuel cell. Cybern. Inf. Technol., 13: 139-147.

Kananai, J. and R. Chancharoen, 2012. Stiff PD and Narma L2 synergy control for a nonlinear mechanical system. Eur. J. Sci. Res., 77: 344-355.

Kandi-D, M., M. Soleymani and A.A. Ghadimi, 2016. Designing an optimal fuzzy controller for a fuel cell vehicle considering driving patterns. Sci. Iranica Trans. B Mech. Eng., 23: 218-227.

Kumar, P., S.K. Kannaiah, S.R. Choudhury and N. Rajasekar, 2017. Genetic algorithm-based modeling of PEM fuel cells suitable for integration in DC microgrids. Electr. Power Compon. Syst., 45: 1152-1160.

Mammar, K. and A. Chaker, 2009. Fuzzy logic control of fuel cell system for residential power generation. J. Electr. Eng., 60: 328-334.

Manikandan, T. and S. Ramalingam, 2016. A review of optimization algorithms for the modeling of proton exchange membrane fuel cell. J. Renewable Sustainable Energy, 8: 1-13.

Nazarian, P. and M.J. Hadidian-Moghddam, 2015. Optimal sizing of a stand-alone hybrid power system using firefly algorithm. Intl. J. Ind. Electron. Electr. Eng., 3: 1-5.

Nells, O., 2001. Nonlinear System Identification: From Classical Approaches to Neural Networks and Fuzzy Models. Springer, Berlin, Germany, ISBN:978-3-662-04323-3, Pages: 786.

Rajasekar, N., B. Jacob, K. Balasubramanian, K. Priya and K. Sangeetha *et al*., 2015. Comparative study of PEM fuel cell parameter extraction using Genetic Algorithm. Ain Shams Eng. J., 6: 1187-1194.

Ren, Y., Z.D. Zhong, H.X. Liu and X.H. Wang, 2012. Particle swarm optimization for identification of PEMFC generation system fuzzy model. Adv. Mater. Res., 589: 260-263.

Rini, D.P., S.M. Shamsuddin and S.S. Yuhaniz, 2011. Particle swarm opti mization: Technique, system and challenges. Int. J. Comput. Appl., 14: 19-27.

Safavi, M., 2013. Application of ABC algorithm for grid-independent hybrid hydro/photovoltaic/ wind/fuel cell power generation system considering cost and reliability. Intl. J. Renewable Energy Res., 3: 928-940.

Sedighizadeh, M., M. Rezaei and V. Najmi, 2011. A predictive control based on neural network for proton exchange membrane fuel cell. World Acad. Sci. Eng. Technol., 5: 395-399.

Seyezhai, R., 2015. Simulation of fuzzy logic controller for PEM fuel cell based hybrid CASCADED multilevel inverter. Electr. Electron. Eng. Intl. J., 4: 63-78.

Swain, P. and D. Jena, 2015. PID control design for the pressure regulation of PEM fuel cell. Proceedings of the 2015 International Conference on Recent Developments in Control, Automation and Power Engineering (RDCAPE'15), March 12-13, 2015, IEEE, Noida, India, ISBN:978-1-4799-7246-3, pp: 286-291.

Zuniga-Ventura, Y., D. Langarica-Cordoba, J. Leyva-Ramos, L. Dýaz-Saldierna and V. Ramýrez-Rivera, 2015. Adaptive back-stepping control for a fuel cell/boost converter system. J. Latex Class Files, 14: 1-11.

Zurada, J.M., 1992. Introduction to Artificial Neural Systems. West Publishing Company, Saint Paul, Minnesot.